Biogeochemistry – Electronic Supplementary Material

Biogeochemical cycling of phosphorus in subsoils of temperate forest ecosystems

Andrei Rodionov[1,2], Sara L. Bauke[1,*], Christian von Sperber[1,3], Carmen Hoeschen[4], Ellen Kandeler[5], Jens Kruse[1,6], Hans Lewandowski[6], Sven Marhan[5], Carsten W. Mueller[4,7], Margaux Simon[1], Federica Tamburini[8], David Uhlig[9,6], Friedhelm von Blanckenburg[9], Friederike Lang[10], Wulf Amelung[1,6]

[1]*Institute of Crop Science and Resource Conservation (INRES) – Soil Science and Soil Ecology, University of Bonn, Nussallee 13, 53115 Bonn, Germany*

[2]*Soil Ecology, University of Bayreuth, Dr.-Hans-Frisch-Str. 1-3, 95448 Bayreuth, Germany*

[3]*Department of Geography, McGill University, 805 Sherbrooke St. W., Montreal QC H3A 0B9, Canada*

[4]*Chair of Soil Science, Department of Ecology and Ecosystem Management, Technical University of Munich, Emil-Ramann-Str. 2, 85350 Freising-Weihenstephan, Germany*

[5]*Institute of Soil Science and Land Evaluation, Soil Biology Department, University of Hohenheim, Emil-Wolff-Str. 27, 70599 Stuttgart, Germany*

[6]*Institute of Bio- and Geosciences – Agrosphere (IBG-3), Forschungszentrum Jülich GmbH, Wilhelm-Johnen-Straße, 52428 Jülich, Germany*

[7]Department of Geosciences and Natural Resource Management, Section for Geography, University of Copenhagen, Øster Voldgade 10, 1350 Copenhagen, Denmark

[8]*Institute of Agricultural Sciences, ETH Zurich, Eschikon 33, 8315 Lindau, Switzerland*

[9]*GFZ German Research Centre for Geosciences, Earth Surface Geochemistry, Telegrafenberg, 14473 Potsdam, Germany*

[10]*Chair of Soil Ecology, University of Freiburg, Bertholdstraße 17, 79085 Freiburg (i. Br.), Germany*

*Corresponding author: sarabauke@uni-bonn.de

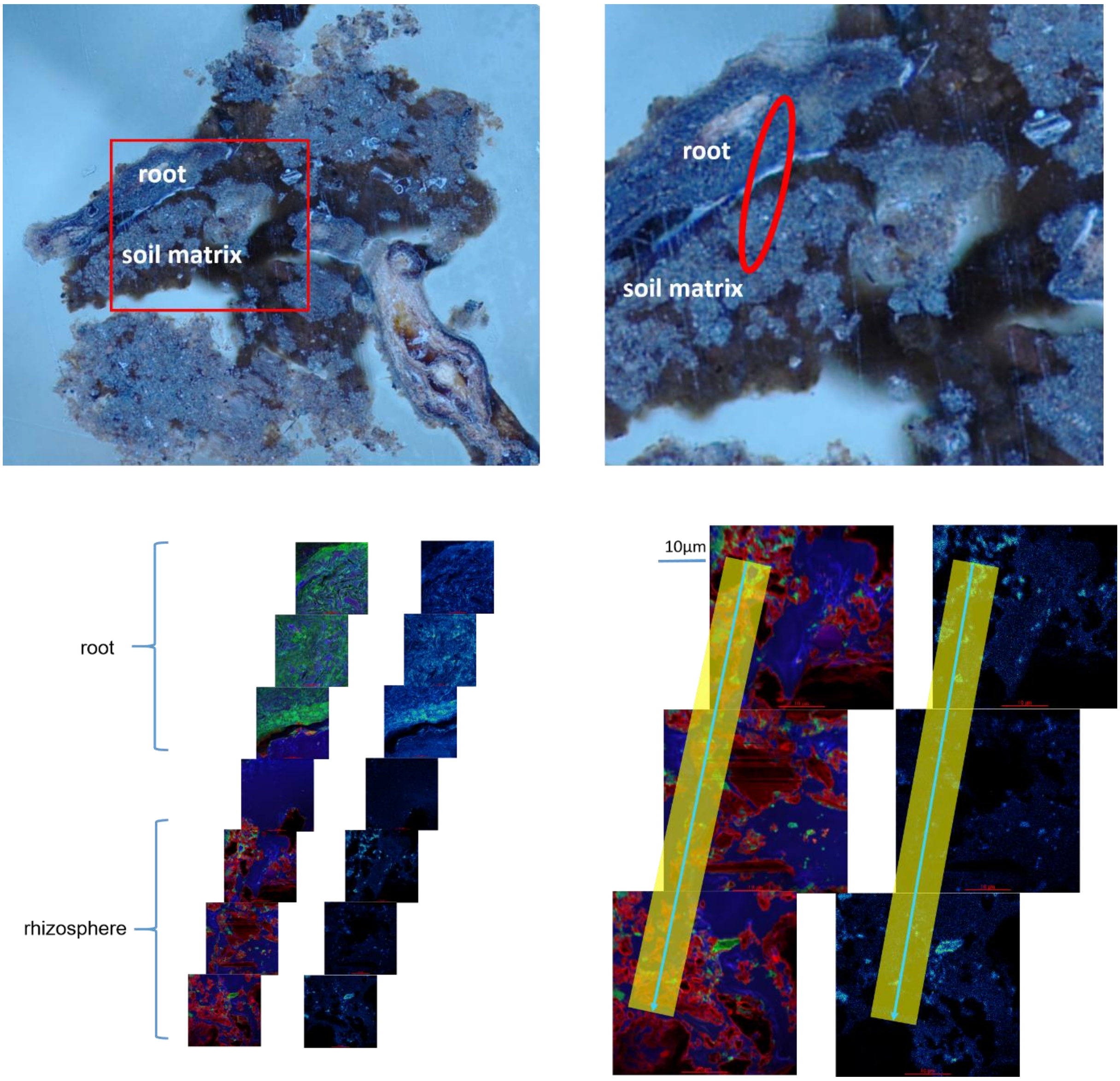

Figure S1. Exemplary work flow for NanoSIMS analysis of VES topsoil sample. Samples were first inspected by optical light microscope in a general view (upper left panel). An area of interest was chosen (indicated by the red box) and inspected in more detail (upper right panel). The red ellipsis indicates the specific area chosen for NanoSIMS analyses. The specific area of interest was first scanned as a transect of 6 to 8 measurements (lower left panel). Finally, ion counts along a line scan within the transect (indicated by the shaded area in the lower right panel) were smoothed and normalized to produce the graphs presented in Figure 2 (main text). For the NanoSIMS images in the lower panels, the left image sequence indicates the distribution of $^{16}O^{-}$ (red) and $^{12}C^{14}N^{-}$ (green) along the transect and the right image sequence indicates the corresponding distribution of $^{31}P^{16}O_2^{-}$, respectively.

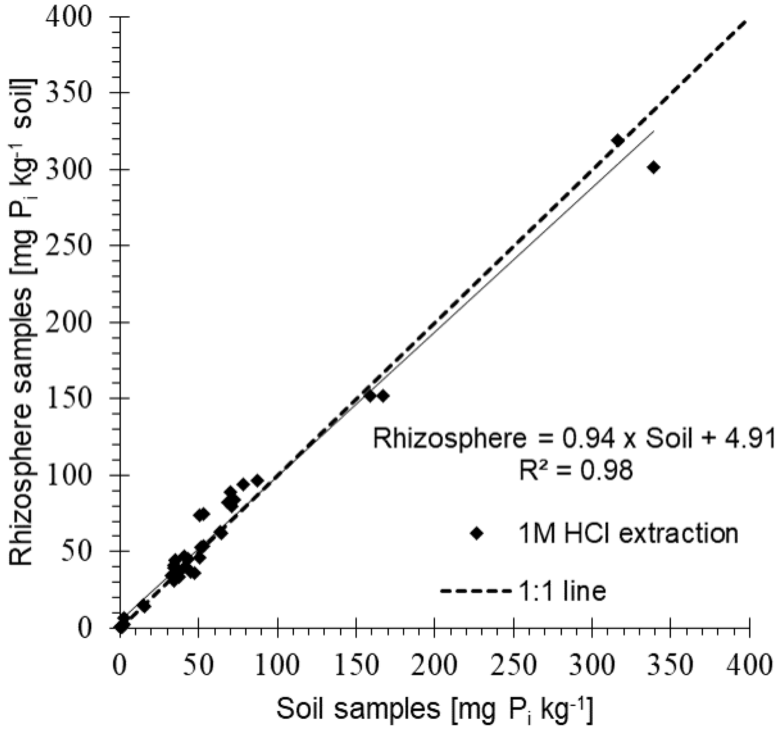

Figure S2. Comparison of inorganic P contents of the 1 M HCl-extractable P fraction in bulk soil and rhizosphere samples.

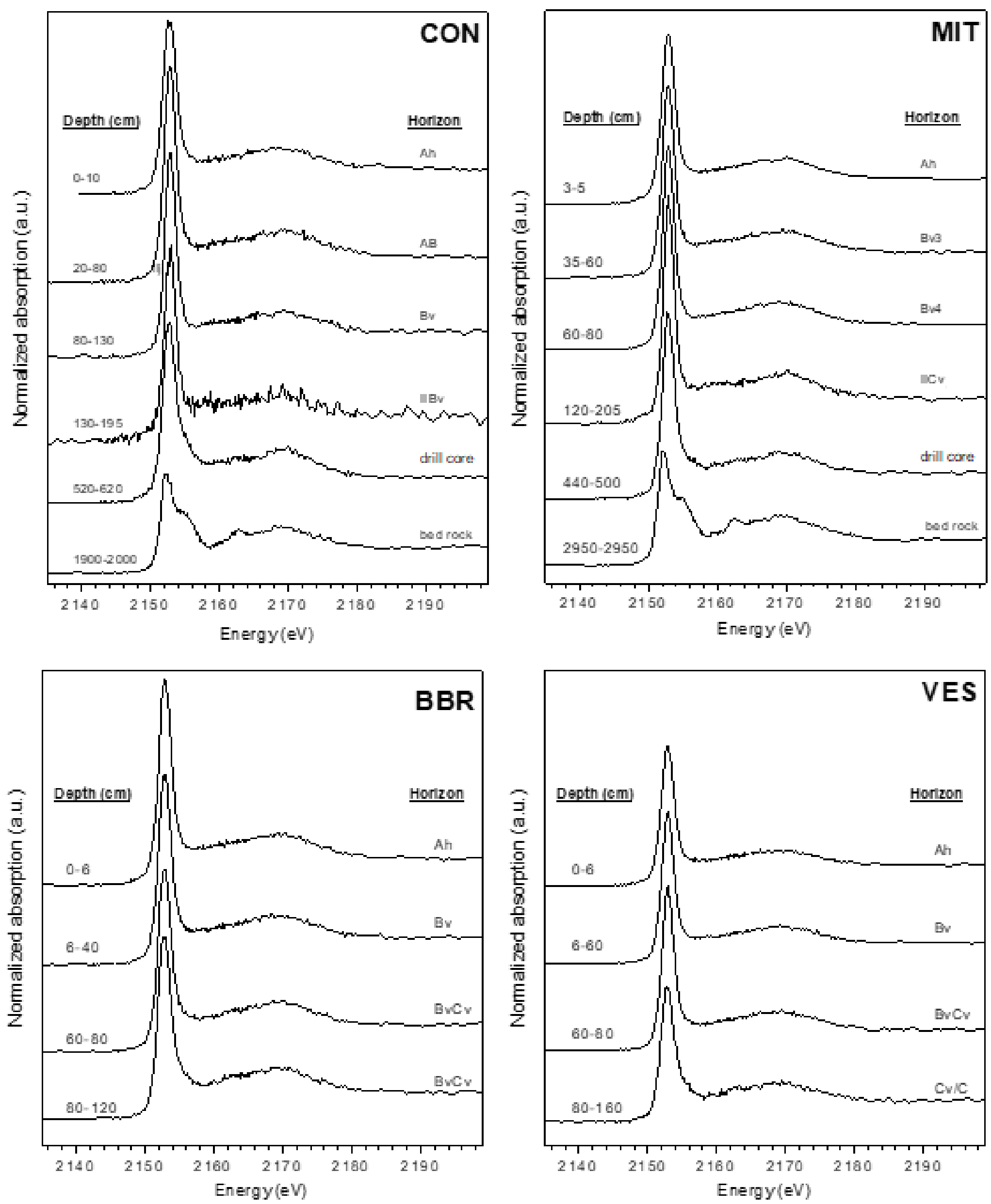

Figure S3. Stacked normalized phosphorus XANES spectra of soils from the four study sites.

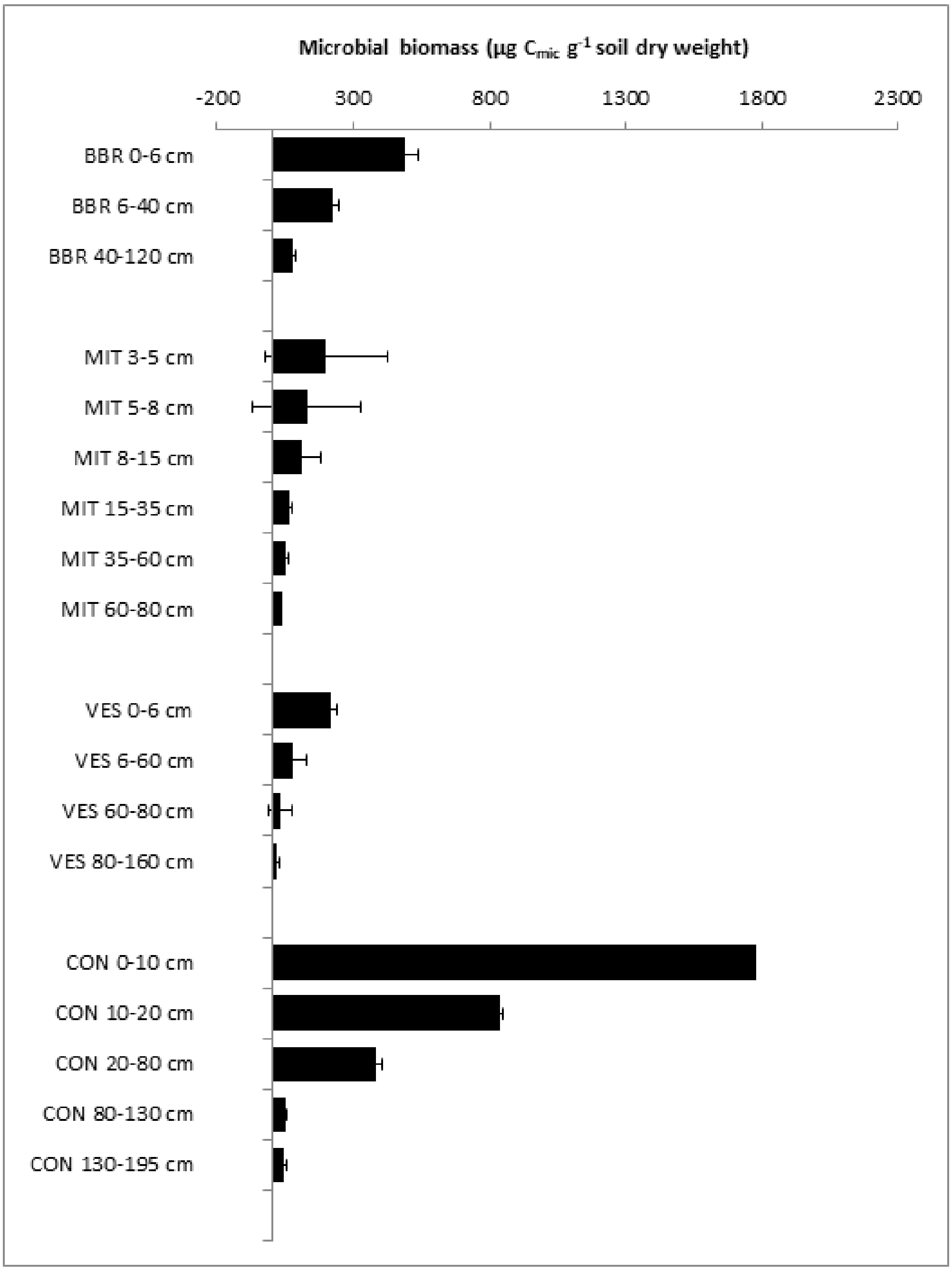

Figure S4. Microbial biomass carbon (C_{mic}) estimated from the maximum initial respiratory response (MIRR) during the initial 9 hours after addition of glucose. C_{mic} (µg C_{mic} g^{-1} soil dry weight) was calculated as C_{mic}=38 ×MIRR (Beck et al. 1997).

Table S1. Drill core profiles with corresponding distribution of Hedley fractions assigned to P-pools in rock and saprolite.

Depth [m]	Total Hedley[1)] [mg P kg^{-1}]	sum-P_i[2)] [mg P kg^{-1}]	sum-P_o[3)] [mg P kg^{-1}]	labile[4)] [mg P kg^{-1}]	moderate labile[5)] [mg P kg^{-1}]	stable[6)] [mg P kg^{-1}]
Mitterfels (MIT)						
2.4	619	600	19	20	96	503
2.6	587	572	15	22	107	458
2.8	911	813	97	47	394	470
2.9 – 3.4 *	2563	1918	645	103	519	1941
3.4 – 3.7 *	16131	4371	11759	165	868	15098
3.7 – 4.2 *	1217	1194	23	57	246	914
4.4 – 5.0 *	2870	2441	429	102	433	2335
5.0 – 5.5	882	867	16	73	223	587
5.5 – 7.8	443	429	13	28	67	348
8.3 – 8.4	487	471	16	35	61	391
9.4 – 9.5 *	2481	2454	27	117	272	2091
12.0 – 13.0	2245	1709	536	84	199	1962
13.0 – 13.8	2000	1784	215	98	248	1654
16.2 – 16.3	413	370	43	21	44	348
17.6 – 17.7	430	426	3	5	16	410
20.0 – 20.1 *	1262	830	433	10	24	1228
26.2 – 26.3	1286	730	556	9	4	1274
28.5 – 28.6	3163	1112	2051	12	5	3146
29.5 – 29.6	5691	4473	1218	22	2	5667
Conventwald (CON)						
2.2	478	436	42	46	143	288
2.4	526	505	21	47	103	376
2.6	581	557	24	41	101	438
2.8	639	613	26	37	88	514
3.0 – 3.7	617	602	15	15	31	572
4.0 – 4.7	786	701	85	19	40	727
4.7 – 5.2	714	684	29	19	40	654
5.2 – 6.2	603	587	16	15	28	560
6.3 – 6.6	661	616	45	21	32	607
10.0 – 11.0	902	657	245	7	3	892
12.9 – 13.0	1477	812	666	6	2	1469
15.1 – 15.3	991	771	220	3	5	983
16.3 – 16.4	1362	797	565	4	3	1355
18.3 – 18.5	1009	804	205	2	0	1007

[1)] Total Hedley = sum of all P fractions in Hedley sequential fractionation.

[2)] sum-P_i = sum of all inorganic P fractions from Hedley sequential fractionation.

[3)] sum-P_o = sum of all organic P fractions from Hedley sequential fractionation.

[4)] labile soil P-pools = sum of resin-P, $NaHCO_3$-P_i, $NaHCO_3$-P_o.

[5)] moderate labile soil P-pools = sum of NaOH-P_i, NaOH-P_o.

[6)] stable soil P-pools = sum of HCl_{dill}-P_i, HCl_{conc}-P_{total}, residual-P.

*Depth intervals marked with asterisks were identified as being from a non-representative source rock as indicated by Zr, Cr, Nb, Ni, Ti concentrations (Uhlig and von Blanckenburg, 2019), but were not excluded here as they are nevertheless relevant for tree nutrient acquisition from the soil profile.